AGU100 ADVANCING EARTH AND SPACE SCIENCE

Radio Science

RESEARCH ARTICLE
10.1029/2018RS006575

Key Points:
- The derivation of total electron content using single-frequency terrestrial GPS receivers and geostationary satellites is demonstrated
- The demonstrated technique is validated by correlation analysis
- The correlations between TEC time series for pairs of receivers and between receivers and an ionosonde over a year show good agreement

Correspondence to:
C. Cooper,
c.a.cooper@bath.ac.uk

Citation:
Cooper, C., Mitchell, C. N., Wright, C. J., Jackson, D. R., & Witvliet, B. A. (2019). Measurement of ionospheric total electron content using single-frequency geostationary satellite observations. *Radio Science*, *54*, 10–19. https://doi.org/10.1029/2018RS006575

Received 12 MAR 2018
Accepted 19 OCT 2018
Accepted article online 24 OCT 2018
Published online 9 JAN 2019

Measurement of Ionospheric Total Electron Content Using Single-Frequency Geostationary Satellite Observations

C. Cooper[1,2], C. N. Mitchell[1], C. J. Wright[1], D. R. Jackson[2], and B. A. Witvliet[1]

[1]Department of Electronic and Electrical Engineering, University of Bath, Bath, UK, [2]Met Office, Exeter, UK

Abstract The ionized upper portion of the atmosphere, the ionosphere, affects radio signals traveling between satellites and the ground. This degrades the performance of satellite navigation, surveillance, and communication systems. Techniques to measure and mitigate ionospheric effects and in particular to measure the total electron content (TEC) are therefore required. TEC is usually determined by analyzing the differential delay experienced by dual-frequency signals. Here we demonstrate a technique which enables TEC to be derived using single-frequency signals passing between geostationary satellites and terrestrial Global Positioning System (GPS) receivers. Geostationary satellites offer the key advantage that the raypaths are not moving and hence are easier to interpret than standard GPS TEC. Daily TEC time series are derived for three ground receivers from Europe over the year 2015. The technique is validated by correlation analysis both between pairs of ground receiver observations and between ground receivers and independent ionosonde observations. The correlation between pairs of receivers over a year shows good agreement. Good agreement was also seen between the TEC time series and ionosonde data, suggesting the technique is reliable and routinely produces realistic ionospheric information. The technique is not suitable for use on every GPS receiver type because drift in derived TEC values was observed for profiles calculated using receivers without links to highly stable clocks. The demonstrated technique has the potential to become a routine method to derive TEC, helping to map the ionosphere in real time and to mitigate ionospheric effects on radio systems.

Plain Language Summary The ionized upper portion of the atmosphere is known as the ionosphere. The ionosphere interferes with signals traveling between satellites and the ground and can cause errors in satellite navigation, surveillance, and communication systems. The impact of these errors can be reduced if we are able to measure the *total electron content* (TEC), which can be simply thought of as the total number of electrons in a straight line between a satellite and the ground. We have developed a technique that allows us to measure TEC using receivers measuring single-frequency signals from geostationary satellites. This is useful because it will increase the number of measurements available and because using geostationary satellites makes the measurements relatively easy to interpret. To test the technique we use a correlation analysis to compare measurements made by the single-frequency receivers. We also correlate technique measurements with independent TEC observations made by an ionosonde. All correlation results showed good agreement, suggesting consistency for the technique, and that the technique is reliable. The demonstrated technique has the potential to become a routine method to derive TEC, which will help to map the ionosphere in real time.

1. Introduction

The ionosphere is the ionized region of the Earth's atmosphere located at altitudes between approximately 80 and 1,000 km. It is created largely through interactions between neutral atmospheric particles and solar radiation. Electromagnetic signals that pass through the ionosphere experience effects, which diminish with increasing radio frequency but are significant below a few gigahertz (GHz) (Hargreaves, 1979). Consequently, understanding the state of the ionosphere is important for maintaining accuracy of Earth-satellite communications and navigation systems.

One such system that is significantly affected by the ionosphere is the Global Positioning System (GPS), which operates at frequencies between 1.1 and 1.6 GHz. To ensure accuracy, ionosphere-dependent corrections must be made to GPSs. The delay experienced by a signal traveling through the ionosphere is proportional to the total electron content (TEC) along the signal path. TEC is the line integral of the electron density of a column through the ionosphere and is calculated along a signal path between a satellite and a

ground-based receiver (Bust & Mitchell, 2008). Consequently, if the signal path from satellite to ground is known, the differential delay experienced by two frequencies of the signal can be used to derive the TEC along the signal path.

Scientific investigations of TEC began with the emergence of artificial satellites as a tool for providing ionospheric measurements (Mendillo, 2006). Using artificial satellites to investigate the ionosphere was first proposed as a method separately by Daniels (1956) and Pfister (1956). First measurements were made by Daniels and Bauer (1959) by analyzing the Faraday rotation of satellite signals. Observations of TEC have been taken for many decades using Faraday rotation from geostationary satellites, where the change in the angle of polarization of a signal traveling from a satellite to the ground is related to the TEC along the path through the ionosphere (Hargreaves, 1979; Ratcliffe, 1972). This technique is less than ideal however, as changes in ionization height can mean approximations made about the state of the local magnetic field become inaccurate and can cause inaccuracies of up to 20% in TEC estimations (Hargreaves, 1992). This occurs as Faraday rotation relates to both the magnetic field strength and the ionization, so the distribution of the ionization along the path can cause an inaccuracy in the TEC estimation.

Since 1992 dual-frequency radio observations have been available as a method for deriving TEC using the GPS network (Mannucci et al., 1999). Dual-frequency observations use the differential temporal delays of phase coherent radio signals to infer values of TEC or the differential phase advance. Dual-frequency receivers can use signals of two different frequencies to remove positioning errors from calculations (Kaplan & Hegarty, 2006). The majority of TEC values today are derived using receivers from GPS networks, which need to account for the ionospheric delay to their signals for optimal accuracy (Bust & Mitchell, 2008). The large global distribution of GPS receivers provides a higher network density for TEC observations than is possible for other ionospheric measurements (such as ionosonde or incoherent scatter radar observations), which combined with high sampling rates results in worldwide coverage of continuous, near-real-time TEC observations (Mannucci et al., 1999; Mendillo, 2006). TEC measurements have been frequently used to analyze the ionospheric storm response, due to the reduced vulnerability of GPS TEC measurements to storm effects when compared to other ionospheric measuring technologies such as ionosondes (Mendillo, 2006).

Geostationary satellite dual-frequency signals have been used recently to derive TEC with dual frequency receivers, such as by Kunitsyn et al. (2015). Geostationary satellite signals have also been used to investigate ionospheric scintillation by Cerruti et al. (2006). Observations made using geostationary satellites and ground receivers are particularly useful, as the point at which the signal intersects the ionosphere (ionospheric pierce point) does not change as it does for nongeostationary satellites (Kunitsyn et al., 2015; Mannucci et al., 1998). By using a geostationary satellite (as opposed to nongeostationary), variations in ionospheric observations can be more accurately attributed to fluctuations of the ionosphere rather than to movement of the satellite. This potentially enables a detailed analysis of the temporal variation of a section of the ionosphere (Kunitsyn et al., 2015).

Here we demonstrate a technique that allows a TEC time series to be derived using the single-frequency signals sent through the satellite-based augmentation system (SBAS) from geostationary satellites to ground-based receivers. Recently, studies such as Hein et al. (2016) have begun to investigate the use of single-frequency signal delays from nongeostationary satellites to estimate TEC. Single-frequency receivers are less expensive than dual-frequency receivers and are thus a preferable data source (Hein et al., 2016).

Our approach to TEC derivation uses single-frequency signals from geostationary satellites, but for the first time this uses the propagation characteristics of the carrier phase advance and the code delay of signals from the Global Navigation Satellite System (GNSS). Several geostationary satellites transmit GNSS signals for the SBASs, including the European Geostationary Overlay System (EGNOS) and the Wide Area Augmentation System (WAAS). These signals are received by several ground-based GNSS receivers on a fixed global network.

This is the first experimental demonstration of TEC derived from a single-frequency GNSS signal from a geostationary satellite. Validation is performed via correlation analysis with ionosonde TEC, and by direct comparison with both ionosonde measurements of foF2, the peak plasma frequency in the *F* region, and ionosonde estimates of TEC over a year. In section 2 the technique is explained. Section 3 describes the sources of GPS receiver and ionosonde data used in this paper, and the existence of clock drift is discussed. Section 4 contains an initial evaluation of the technique, comparing daily profiles from three receivers and daily profiles from a nearby ionosonde. The initial data checks performed prior to more thorough

validation are also discussed. The method is further validated using statistical correlation in sections 5 and 6. In section 5 the TEC time series obtained from three independent GPS ground receivers are correlated with each other. Section 6 performs further correlation analysis between TEC profiles from the demonstrated technique and independent ionosonde observations. Section 7 provides a brief discussion and concluding statements.

2. Introduction of the Technique

2.1. Method

Geostationary satellites are used to relay information for the GNSS SBAS. These signals transmit on the same frequencies as the standard GPS L1 signal, with the geostationary satellites relaying a signal uplinked from a ground location. These signals will experience a phase advance and an excess group delay that is dependent upon the state of the ionosphere. The pseudorange (or perceived range) of a GPS signal is related to the ionospheric delay as shown in equation (1) (Davies, 1990; Hargreaves, 1992; Mannucci et al., 1999; Sardon et al., 1994).

$$P_1 = \rho + d_{tropo} + \frac{40.3 \times I}{f_1^2} + c\left(\tau_1^r - \tau_1^s\right). \tag{1}$$

Here P_1 represents the GPS pseudorange (in meters), ρ is the real satellite to ground distance (in meters), d_{tropo} is the distance bias caused by the signal delay originating in the troposphere (in meters), I is the TEC along the signal path (in electrons per square meters), f_1 is the signal frequency (in Hertz), c is the speed of light in a vacuum, and τ_1^r and τ_1^s represent dispersive delays caused by the hardware of the receiver and satellite respectively (in seconds) of the receiver and satellite, respectively. These component biases for the pseudorange delay include satellite and receiver clock errors, satellite and receiver hardware delays, multipath, and measurement noise. The units of the constant 40.3 are in cubic meters per square second.

The carrier phase range, L_1, (in meters) can be expressed as shown in equation (2) (Davies, 1990; Mannucci et al., 1999; Sardon et al., 1994).

$$L_1 = \rho + d_{tropo} - \frac{40.3 \times I}{f_1^2} - \lambda_1 n_1 + c\left(\varepsilon_1^r - \varepsilon_1^s\right) \tag{2}$$

Here λ_1 is the carrier wavelength (in meters), n_1 represents the associated biases of the receiver and satellite (Sardon et al., 1994), ε_1^r and ε_1^s are dispersive hardware delays from the receiver and satellite, respectively, and other variables are as defined previously. These component biases for the carrier phases include an integer ambiguity term that represents number of phase cycles, satellite and receiver clock errors, satellite and receiver hardware delays, multipath, and measurement noise. In Leick (2004) the clock biases are independent for each component, but here they have been combined to follow Mannucci et al. (1999). The pseudorange and phase range can be differenced to reveal the excess ionospheric path. This ionospheric path relates directly to the relative TEC:

$$P_1 - L_1 = 2\frac{40.3 \times I}{f_1^2} + \lambda_1 n_1 + c\left(\tau_1^r - \tau_1^s\right) - c\left(\varepsilon_1^r - \varepsilon_1^s\right). \tag{3}$$

Rearranging equation (3) gives equation (4).

$$I = \frac{f_1^2}{2 \times 40.3} \times \left(P_1 - L_1 - \lambda_1 n_1 - c\left(\tau_1^r - \tau_1^s\right) + c\left(\varepsilon_1^r - \varepsilon_1^s\right)\right) \tag{4}$$

The terms $\tau_1^r, \tau_1^s, \varepsilon_1^r, \varepsilon_1^s$, and n_1 in equation (4) cause a constant offset in TEC that does not vary with time. As geostationary satellites used here are at a fixed height multipath effects will remain constant. Therefore,

$$I_{rel} = \frac{(P_1 - L_1) \times f_1^2}{2 \times 40.3}. \tag{5}$$

I_{rel} is an uncalibrated measurement of the absolute TEC, known as the relative TEC (in electrons per square meter), where 1 TEC units (TECU) is equivalent to 10^{16} electrons per square meter (Mannucci et al., 1998).

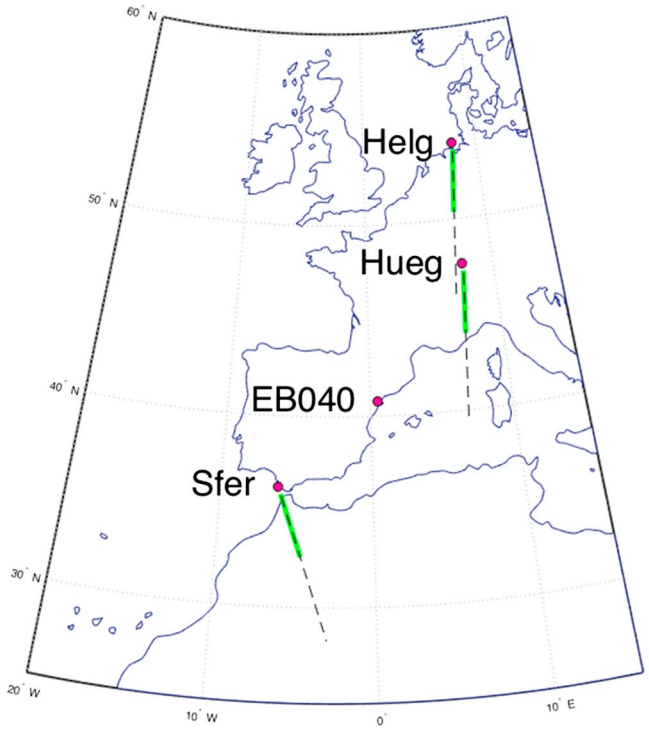

Figure 1. Locations of Global Positioning System receivers (Helg, Hueg, and Sfer) and Roquetes ionosonde (EB040). The section of the paths between the satellite (SES-5) and 80- and 400-km altitude are indicated with green lines and the section path from 80 to 1,000 km with black dashed lines.

3. Validation Data Sources

3.1. GPS Receiver Data

To validate the technique data from three ground-based receivers capable of receiving geostationary signals are used. Two of these receivers are located in Germany, one in Heligoland (54.10°N, 7.53°E) and the other in Huegelheim (47.50°N, 7.35°E). The third receiver is located in San Fernando in Spain (36.28°N, 6.12°W). These receivers will be referred to as Helg, Hueg, and Sfer, respectively throughout the study. One of the GPS receivers (Helg) is part of the EUREF Permanent GNSS Network, while the other two (Hueg and Sfer) are part of the International GNSS Service (IGS). The sampling rate of the GPS TEC data is 30 s, and the data were evaluated using the equations in section 2. The satellite from which signals were sent to the ground receivers in this research is the SES-5 (or Sirius 5) geostationary satellite (PRN 136), positioned at 5°E.

3.2. Ionosonde Data

Ionosonde data were identified as a source of ionospheric observations that were independent from the satellite derived TEC and could thus be used for validation. Ionosondes are active instruments that transmit and receive high-frequency radio signals. By repeatedly reflecting radio waves off the ionosphere and analyzing the return signal, ionosondes can obtain vertical time series of the plasma frequency and hence derive values of electron density. Ionosonde TEC is a combination of measured and modeled values. The electron density up to the height of peak plasma frequency is measured by the ionosonde, and from this point up to a height of 1,000 km the values are modeled using the observed values (Huang & Reinisch, 2001; McKinnell et al., 2007; Reinisch & Huang, 2001). The TEC value of a column through the whole ionosphere is then found by adding the integral of electron density through the measured section to the integral of electron density through the modeled section (Huang & Reinisch, 2001; McKinnell et al., 2007). For the ionosonde data used here the ionosphere above the peak is modeled using a Chapman profile with a constant scale height.

The three GPS receivers were selected from a network of receivers across Europe. The geometrical configuration of the satellite to receiver paths are such that they can be compared to the ionosonde in Roquetes, Spain (40.80°N, 0.50°E) for validation. Ionosonde data used in this paper were obtained from the Digital Ionogram Data Base (DIDbase; Reinisch & Galkin, 2011). The Roquetes ionosonde is also referred to by the station code, EB040. The locations of the receivers and ionosondes are shown on the map in Figure 1, along with the satellite and corresponding measurement paths between the receiver and the geostationary satellite. The sections of the measurement paths that intersect the ionosphere between 80- and 400-km altitude are indicated in Figure 1 by a solid green line, and the black dashed line indicates the ionospheric intersect between 80 and 1,000 km.

3.3. The Impact of Clock Drift

Errors in single-frequency GPS TEC derivation can arise from *clock drift*, which is the drift in the inbuilt clock of the terrestrial receiver (Mannucci et al., 1999). Of the three receivers used in this study, one has an oscillator that is linked to an atomic clock and thus should be minimally vulnerable to this issue, but clock drift must be accounted for with the other two. The Helg and Hueg receivers both have oscillators that do not have an atomic clock, while the Sfer receiver has an oscillator that does have an atomic clock. Noticeable clock drift was observed in the 24-hour time series plots derived from the Helg and Hueg receivers but was far less noticeable in profiles derived from Sfer.

Figure 2 shows the clock drift observed in the GPS derived daily TEC time series for each of the three receivers before detrending. This results in a noticeable diagonal tilt over a 24-hour time series for two of the receivers. This was corrected for using a linear detrend, which removed a different amount of drift each day. It can be seen that there is little noticeable drift in the profile from the Sfer receiver, which is linked to an atomic clock.

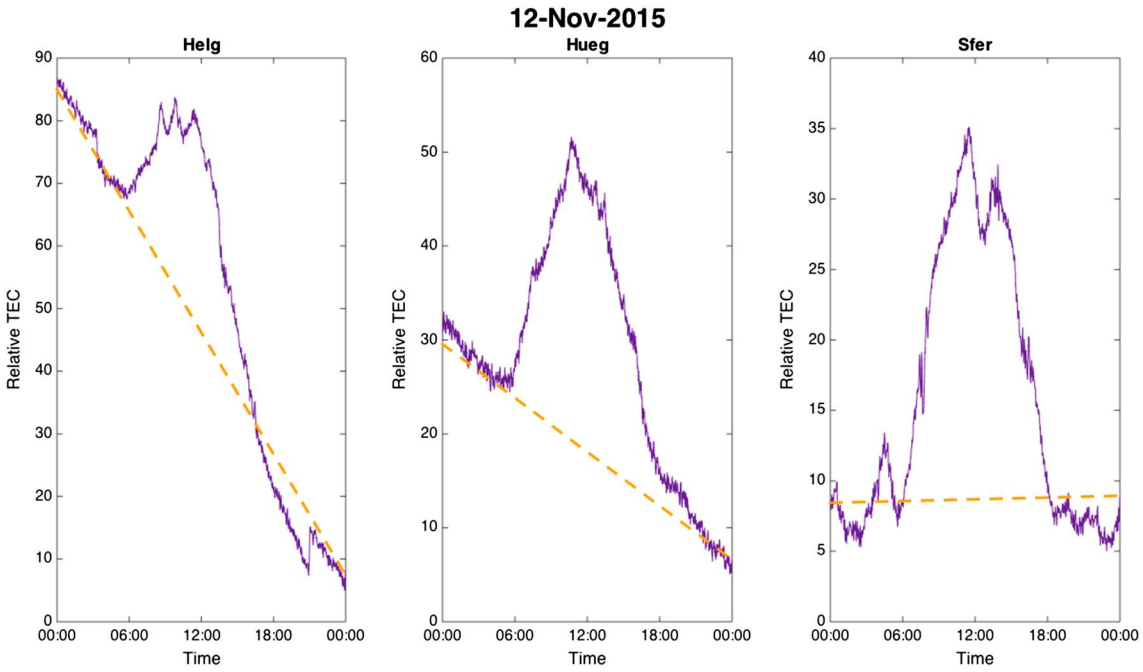

Figure 2. Predetrended derived daily relative TEC profiles from the Sfer, Helg, and Hueg receivers.

However, the profiles from both Helg and Hueg, which are not linked to atomic clocks, show noticeable clock drift. Investigation into this drift suggested that a drift of approximately 43 and 15 ns was observed over a 24-hour period for these two receivers, assuming that the TEC is not changing significantly day to day. Further research will be conducted to assess the importance of this clock drift and attempt to mitigate any problems it causes. Hein et al. (2016) also experienced issues with clock drift in their study into single-frequency TEC derivations from GPS satellites.

4. Initial Evaluation of the Technique

For each of the three receivers diurnal TEC time series were calculated for each day in 2015 using the demonstrated technique. Figure 3 shows the daily TEC time series, for example, days generated by the demonstrated technique, for all three GPS receivers and additionally foF2 from the Roquetes ionosonde; foF2 is a directly measured value that corresponds to the maximum electron density in the ionosphere. Ionosondes are also capable of producing TEC values, as shown, but these contain a modeled component as the region of the ionosphere above the peak electron density cannot be observed by an ionosonde. The Helg and Hueg receivers are located to the north east of the ionosonde, while the Sfer receiver is located south west of the ionosonde.

These plots indicate a good level of agreement in the diurnal variations and in some shorter-term variations between the three ground receivers and between the receivers and the ionosonde. Note that the ionosonde produces an estimate of vertical TEC in the ionosphere, whereas the Geostationary GPS (GPS GEO) produces slant TEC through the ionosphere and the plasmasphere. The plasmasphere should account for a few TECU. Using a geometrical correction the slant to equivalent vertical TEC correction factor (Leitinger et al., 1975) for the ionosphere is 0.47 (Helg), 0.59 (Heug), and 0.74 (Sfer) for the satellite elevations. Taking these into account the magnitude of the diurnal TEC variations observed with the GPS GEO method are comparable to those from the ionosonde. It should also be noted that the conversion factor from slant to equivalent vertical TEC for a geostationary satellite viewed from a fixed receiver is a fixed value and hence will not affect the correlation results presented later in this paper.

This visual inspection suggests that the technique performs well for all four GPS-GEO examples. It should be emphasized that only the relative TEC changes should be considered here. The offsets seen between the relative TEC values derived from the three receivers are caused by differences in receiver hardware ($\tau_1^r, \varepsilon_1^r,$

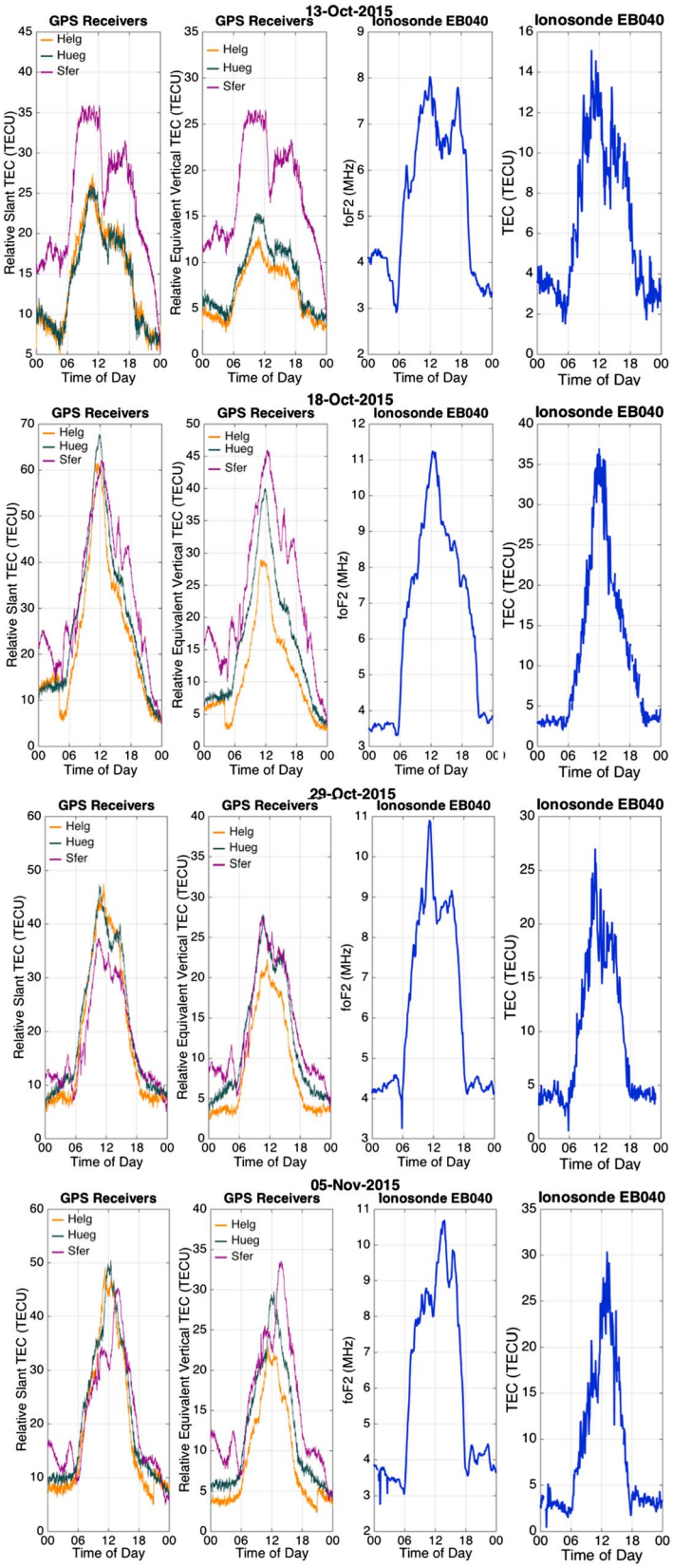

Figure 3. Relative TEC time series derived using the demonstrated technique at the Helg, Hueg, and Sfer ground receivers and observed foF2 time series and derived TEC from the Roquetes ionosonde from 13, 18, 29 October and 5 November 2015.

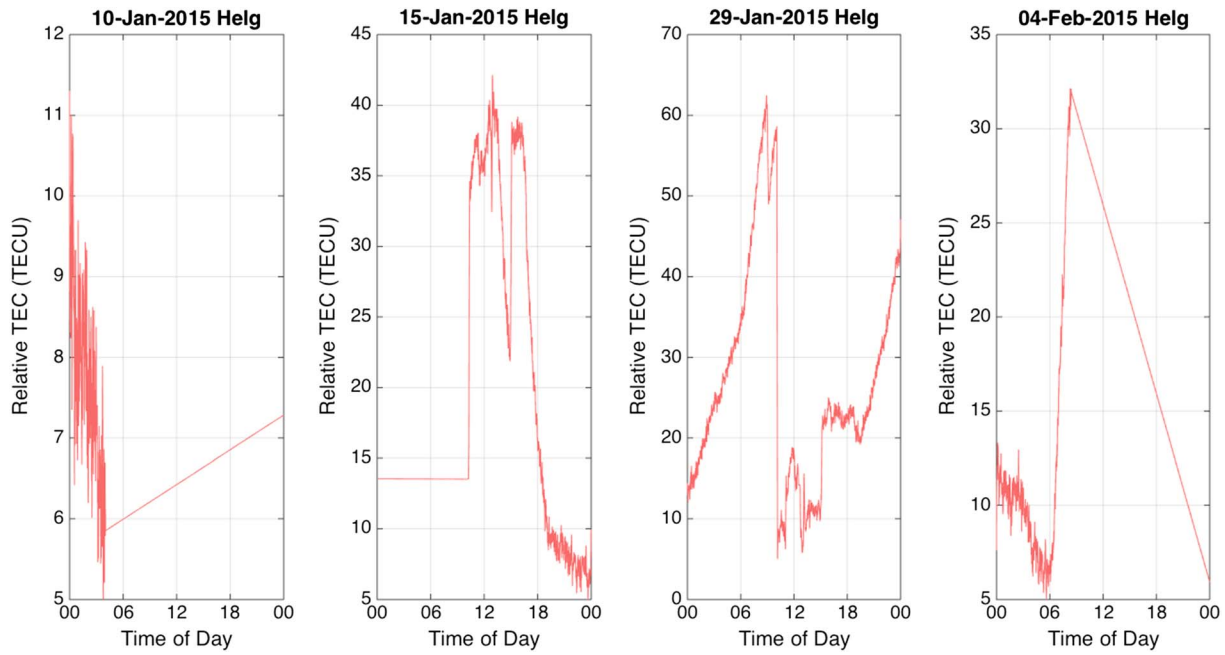

Figure 4. Examples of unrealistic time series derived using the demonstrated technique, which were discarded to prevent contamination of the verification data set.

and n_1 in equation (4)), and the minimum of the GPS-GEO value each day has been set to a value of 5 TECU for plotting purposes.

4.1. Preliminary Inspection of Relative TEC Time Series

For quality control purposes all time series generated using the demonstrated technique were visually inspected. Those that were judged unrealistic because they were either contaminated by substantial losses of lock or because they were incomplete days were discarded to avoid contamination of the data set used for validation. A day was discarded if it met any of the following criteria: (1) diurnal TEC pattern absent due to phase jumps (2) more than 15% of data missing, (3) large discontinuities in TEC time series, (4) and one constant TEC value over a 24-hour period (i.e., no data). Figure 4 shows examples of time series derived using the demonstrated technique at the Helg receiver for days that were discarded.

From Figure 4 it can be seen that time series often become unrealistic if the receiver loses lock (where a near-instantaneous large jump in *y*-axis value occurs) at any point in the day. Lock is lost when the terrestrial receiver cannot detect the signal from the satellite and can be near instantaneous or last for a few minutes. Lock can be lost in the presence of ionospheric scintillation or when the amplitude of the signal changes (Leick, 2004). The number of days in 2015 that were discarded for each station are listed in Table 1. It is acknowledged that the number of days discarded is high but considered acceptable for this proof of concept.

5. Correlation Analysis

5.1. Analysis Between TEC Time Series

The agreement between time series obtained from three GPS receivers was assessed using a correlation analysis over a year's worth of data for the year 2015. For each combination of receivers, a 24-hour TEC time series from one receiver was correlated with the 24-hour time series from the second receiver for the same day. The two time series were interpolated from 30-second onto a 1-minute time scale, then overlaid, and the correlation was calculated to find a measure of the agreement between them. Next, one time series was fixed, and the other was shifted in 1-min time steps. A correlation value was calculated between the fixed and shifted time series after each shift for shifts extending up to 180 min. The percentage of days each correlation value was

Table 1
Days Discarded for Each GPS Receiver for the Year 2015

Station	Number of days discarded
Helg	126 (35%)
Hueg	115 (32%)
Sfer	241 (66%)

Table 2
Days Included in Each GPS Pair Analysis

Station one	Station two	Number of days included
Sfer	Helg	101
Sfer	Hueg	112
Helg	Hueg	211

measured for each shift was then computed and represented with a color scale.

The TEC time series for each GPS receiver were correlated with the time series derived for each of the other two receivers, with days discarded as explained in Figure 4. Table 2 lists the number of days included in each receiver pair analysis after invalid time series were discarded.

Figure 5 shows the results from the correlation analysis for each pair of GPS receivers. In these correlation plots each pixel represents the percentage of data recorded, with lag on the *x* axis and correlations on the *y* axis. A year's worth of data is displayed in each plot, with each day providing a single correlation value for each lag value. The majority of the correlations calculated were between 0.8 and 0.9. Anticorrelations were negligible in number and thus only positive correlations are shown.

High correlations are seen between all pairs of GPS stations, peaking around a lag of 0 (when both time series are overlaid for the same time). Correlations are lower at lags moving away from 0. This is consistent with expectations, as at these lags there is a significant time difference between the two time series being correlated. Figure 5 shows that the correlations are higher between Helg and Hueg (panel a) than for either of the correlation pairs involving Sfer (panels b and c). This is to be expected, as the Sfer receiver is geographically further away from both Helg and Hueg than they are from each other. This means that correlations between Sfer and other stations will be high for a shorter time and lower at large lags.

It can be seen in Figure 5 that there is a slight offset from 0 for the lag at which peak correlation values are attained, most noticeably for correlations involving Sfer. As electron density in the ionosphere is dependent upon solar radiation, the time of day at which peak density occurs will correspond with local solar noon time at the observing receiver location. Consequently, the time series will correlate best when the local solar noon of each time series are aligned, which as these data are in UTC will cause an offset. Peak values are reached at a lag close to corresponding local time difference, suggesting the offset is mostly due to local time difference.

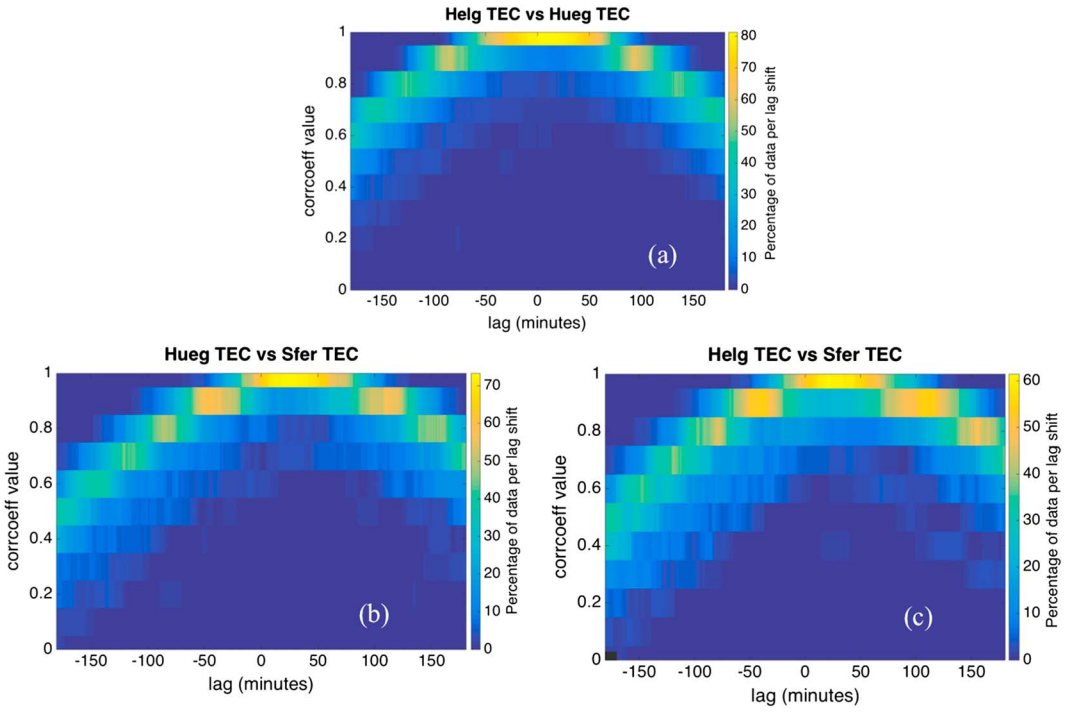

Figure 5. Correlation analysis of daily Global Positioning System-derived relative TEC time series from pairs of GPS receivers, (a) Helg versus Hueg, (b) Hueg versus Sfer, and (c) Helg versus Sfer, for all usable days in 2015.

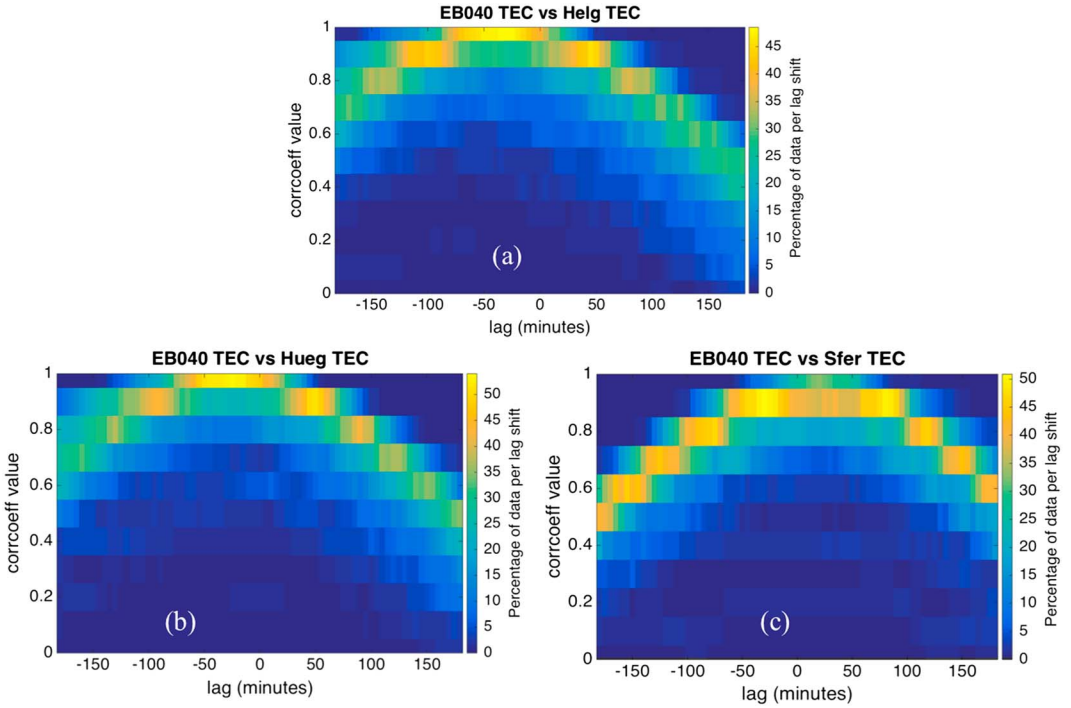

Figure 6. Daily correlations between relative TEC from the three Global Positioning System receivers and the Roquetes ionosonde, (a) EB040 versus Helg, (b) EB040 versus Hueg, and (c) EB040 versus Sfer, for all usable days in 2015.

6. Ionosonde TEC to GPS TEC

Daily time series of GPS TEC from the three receivers were each correlated with daily time series of ionosonde TEC from the Roquetes ionosonde. Ionosonde TEC values were used rather than foF2 so correlations were between as similar parameters as possible. However, it is also to be noted that TEC is a derived quantity from the ionosonde. Correlations were found for the year 2015 using the same process as described in section 5.1, but with the GPS data downsampled onto a 5-min timescale to match the ionosonde sampling rate. The results are shown in Figure 6. Only positive correlations are shown, as anticorrelations were negligible in number.

Correlations are high between the ionosonde and all three receivers; however, peak correlations are slightly lower between the ionosonde and Sfer (panel c) than for the other two receivers. While Sfer is the closest of the three receivers to the ionosonde at the Earth's surface, the satellite to receiver measurement paths for Helg and Heug are closer to the ionosonde's measurement path in the ionosphere than for Sfer (see Figure 1).

It can be seen from Figure 6 that the peak correlation is offset from zero lag for all three receivers. This shift implies that the ionosonde time series correlates best with GPS time series from earlier or later times (plots imply a shift of 30–50 min). This shift is probably the result of the movement of the sun as the lag delay matches up approximately with the local time difference between the receivers and the ionosonde. Sfer (panel c) also shows a broader temporal peak in lag. The high correlations seen in all three plots imply a consistent, good agreement between the ionosonde observed profiles, and the GPS-derived profiles over a year.

7. Discussion and Conclusions

A technique has been demonstrated that allows daily relative TEC time series to be derived using a single-frequency signal transmitted from a geostationary satellite to a ground-based receiver. Initial analysis through visual inspection of the slant TEC shows that the time series produced similar diurnal variations at three ground receivers in Europe. Some of the short-term features were also similar. Statistical correlations were calculated between pairs of 24-hour TEC time series for the same day from different ground receivers. The results show strong agreement (correlations above 0.9), with shifts in the lag at which peak correlation is

reached occurring mostly due to local time difference. Analysis between daily time series generated by the GPS GEO technique and daily time series of TEC observed by the Roquetes ionosonde showed high correlations consistently over a year. A shift in the time at which peak correlations were seen was observed due to local time differences.

Further refinement of the technique is needed to automatically and reliably reject discontinuous or missing data streams and in some cases to resolve issues by fixing cycle slips. A potential source of error in the demonstrated technique arises from clock drift. One of the three receivers used in this study was linked to an atomic clock, but the other two were not. The receivers lacking an atomic clock link experienced a timing drift of tens of nanoseconds over a 24-hour period. This drift was noticeable in the raw derived time series, but a linear detrending these results allowed the clock drift to be removed and final time series to be produced. Higher-order terms in clock drift would have an effect on the correlations; however, by visual inspection of drift in Figure 3 it appears that clock drift is not causing a significant deterioration in end results. Clock drift will be investigated further across different GPS receiver types following this study to fully assess its impact and identify potential mitigations.

The demonstrated technique offers significant advantages as a data source for ionospheric mapping because it provides a time series of relative TEC from fixed elevation and azimuth paths through the ionosphere. It is anticipated that future research will quantify the benefit of this data for ionospheric data assimilation.

Acknowledgments

C. Cooper is supported by the Systems Centre, the EPSRC-funded Industrial Doctorate Centre in Systems (Grant EP/G037353/1) and the Met Office. C. J. Wright is funded by a Royal Society Research Fellowship, ref UF160545 and by Natural Environment Research Council grant NE/R001391/1. C. N. M is supported through NERC fellowship NE/P006450/1. GPS data were provided by the EUREF Permanent GNSS Network (Bruyninx et al., 2012) and The International GNSS Service (IGS; Dow et al., 2009); data are available at http://sopac.ucsd.edu. Ionosonde data were provided by the Lowell Digital Ionogram DataBase (DIDBase; Reinisch & Galkin, 2011) available online at http://giro.uml.edu/didbase/scaled.php. The authors thank David Altadill of the Ebre Observatory for the use of ionosonde data.

References

Bruyninx, C., Habrich, H., Söhne, W., Kenyeres, A., Stangl, G., & Völksen, C. (2012). Enhancement of the EUREF permanent network services and products. *International Association of Geodesy Symposia*, *136*, 27–34. https://doi.org/10.1007/978-3-642-20338-1_4

Bust, G. S., & Mitchell, C. N. (2008). History, current state, and future directions of ionospheric imaging. *Reviews of Geophysics*, *46*, RG1003. https://doi.org/10.1029/2006RG000212

Cerruti, A. P., Ledvina, B. M., & Kintner, P. M. (2006). Scattering height estimation using scintillating wide area augmentation system/satellite based augmentation system and GPS satellite signals. *Radio Science*, *41*, RS6S26. https://doi.org/10.1029/2005RS003405

Daniels, F. B. (1956). *Electromagnetic propagation studies with a satellite vehicle*, *Scientific uses of Earth Satellites*. (J. A. van Allen, Ed.), (Chap. 30, pp. 276–282). Ripol Classic. London: University of Michigan Press/ Chapman and Hall.

Daniels, F. B., & Bauer, S. J. (1959). The ionospheric Faraday effect and its applications. *Journal of the Franklin Institute*, *267*(3), 187–200. https://doi.org/10.1016/0016-0032(59)90133-4

Davies, K. (1990). *Ionospheric radio* (Vol. 31). London, UK: Peter Peregrinus Ltd.

Dow, J. M., Neilan, R. E., & Rizos, C. (2009). The International GNSS Service in a changing landscape of Global Navigation Satellite Systems. *Journal of Geodesy*, *83*(3–4), 191–198. https://doi.org/10.1007/s00190-008-0300-3

Hargreaves, J. K. (1979). *The upper atmosphere and solar-terrestrial relations*. Wokingham, Berkshire, England: Van Nostrand Reinhold Company Ltd.

Hargreaves, J. K. (1992). *The solar-terrestrial environment*. Cambridge: Cambridge University Press. https://doi.org/10.1017/CBO9780511628924

Hein, W. Z., Goto, Y., & Kasahara, Y. (2016). Estimation method of Ionospheric TEC distribution using single frequency measurements of GPS signals. *International Journal of Advanced Computer Science and Applications*, *7*(12), 1–6.

Huang, X., & Reinisch, B. W. (2001). Vertical electron content from ionograms in real time. *Radio Science*, *5*(1), 335–342. https://doi.org/10.1038/srep11648

Kaplan, E. D., & Hegarty, C. J. (2006). *Understanding GPS: Principles and applications* (2nd ed.). Norwood, MA: Artech House.

Kunitsyn, V. E., Padokhin, A. M., Kurbatov, G. A., Yasyukevich, Y. V., & Morozov, Y. V. (2015). Ionospheric TEC estimation with the signals of various geostationary navigational satellites. *GPS Solutions*, *20*(4), 877–884. https://doi.org/10.1007/s10291-015-0500-2

Leick, A. (2004). *GPS satellite surveying* (3rd ed.). Hoboken, NJ: John Wiley & Sons.

Leitinger, R., Schmidt, G., & Tauriainen, A. (1975). An evaluation method combining the differential Doppler measurements from two stations that enables the calculation of the electron content of the ionosphere. *Zeitschrift Fuer Geophysik*, *41*, 201–213.

Mannucci, A. J., Iijima, B. A., Lindqwister, U. J., Pi, X., Sparks, L., Wilson, B. D., & Mannucci, T. (1999). In W. R. Stone (Ed.), *GPS and ionosphere*, *Review of Radio Science*. Pasadena, CA: Jet Propulsion Laboratory. Retrieved from https://trs.jpl.nasa.gov/bitstream/handle/2014/16838/99-0242.pdf?sequence=1

Mannucci, A. J., Wilson, B. D., Yuan, D. N., Ho, C. H., Lindquister, U. J., & Runge, T. F. (1998). A global mapping technique for GPS-derived ionospheric total electron content measurements. *Radio Science*, *33*(3), 565–582. https://doi.org/10.1029/97RS02707

McKinnell, L. A., Opperman, B., & Cilliers, P. J. (2007). GPS TEC and ionosonde TEC over Grahamstown, South Africa: First comparisons. *Advances in Space Research*, *39*(5), 816–820. https://doi.org/10.1016/j.asr.2006.10.018

Mendillo, M. (2006). Storms in the ionosphere: Patterns and processes for total electron content. *Reviews of Geophysics*, *44*, RG4001. https://doi.org/10.1029/2005RG000193.CONTENTS

Pfister, W. (1956). *Study of fine structure and irregularities of the ionosphere with rockets and satellites*, *Scientific uses of Earth Satellites* (J. A. van Allen, Ed.), (Chap. 31). Ripol Classic. Ann Arbor, MI: University of Michigan Press.

Ratcliffe, J. A. (1972). *An introduction to the ionosphere and magnetosphere*. London: Cambridge University Press.

Reinisch, B. W., & Galkin, I. A. (2011). Global Ionospheric Radio Observatory (GIRO). *Earth, Planets and Space*, *63*(4), 377–381. https://doi.org/10.1109/URSIGASS.2011.6050896

Reinisch, B. W., & Huang, X. (2001). Deducing topside profiles and total electron content from bottomside ionograms. *Advances in Space Research*, *27*(1), 23–30. https://doi.org/10.1016/S0273-1177(00)00136-8

Sardon, E., Rius, A., & Zarraoa, N. (1994). Estimation of the transmitter and receiver differential biases and the ionospheric total electron content from global positioning. *Radio Science*, *29*(3), 577–586. https://doi.org/10.1029/94RS00449